J. Appl. Comput. Mech., 7(SI) (2021) 1009-1019
DOI: 10.22055/JACM.2020.32927.2104
ISSN: 2383-4536
jacm.scu.ac.ir

Shahid Chamran University of Ahvaz

Journal of Applied and Computational Mechanics

Research Paper

Natural frequencies and internal resonance of beams with arbitrarily distributed axial loads

Stefano Lenci[1], Francesco Clementi[1]

[1]Department of Civil and Building Engineering and Architecture, Polytechnic University of Marche, 60131 Ancona, Italy, Email: lenci@univpm.it

[2]Department of Civil and Building Engineering and Architecture, Polytechnic University of Marche, 60131 Ancona, Italy, Email: francesco.clementi@univpm.it

Received March 12 2020; Revised May 22 2020; Accepted for publication July 08 2020.
Corresponding author: Stefano Lenci (lenci@univpm.it)

Abstract. An exact analytical solution for transversal free vibrations of a beam subjected to an arbitrary distributed axial load and a tip tension is obtained by means of a power series representation, whose coefficients are determined recursively in an easy way. The dependence on the natural frequencies on the load is then investigated, and the buckling load (corresponding to vanishing frequency) is also discussed. Next, the 1:3 internal resonance between the first and the second mode is deeply studied, and an interesting (and unexpected) property is found for linearly distributed axial loads.

Keywords: Heavy beams, vertical risers, internal resonance, distributed loads, exact analytical solution.

1. Introduction

The problem of transversal vibrations (and static buckling) of a beam with a distributed axial load, and possibly a tip force in the axial direction, is interesting and find applications in vertical risers [1, 2, 3, 4], rotating blades [5], tall slender structures subjected to their own weight (trees [6], obelisks [7], slender skyscrapers, etc.) and in many other engineering applications. For an overview on the problem the reader is referred to [8].

The effect of a concentrated axial force, acting on the boundary of the beam, on the natural frequencies has been considered in classical references [9] and textbooks [10, 11]. Here, because of the absence of the distributed axial load, the solution can be obtained in closed form for all boundary conditions [12]. Comparison of different theoretical results (beam theory, FEM and Ritz method) is reported in [13], where also an episodic experimental result is presented. More systematic and extended experiments, and a comparison with numerical computations, are the subject of [14].

Much more demanding is the case with a distributed axial load. According to Love [15], Art. 276, and Villaggio [16], pag. 256, the *static buckling* load of a beam with *uniformly* distributed axial load has been solved for the first time by Greenhill [17], which obtained a closed form solution using Bessel functions.

The problem of *transversal vibrations* of beam subjected to a distributed axial load, which is even more difficult, has been addressed by various authors. Laird and Fauconneau [18] obtained upper and lower bounds for natural frequencies. Similarly, Pilkington and Carr [19] obtained an approximate solution starting from the Rayleigh quotient. Kim [20] found a closed form approximate analytical solution by using the WKB method.

Sparks [21] obtained an elaborated approximate analytical solution exploiting the known solution for cables (i.e. strings). As a matter of fact, he also reported the exact solution, in terms of Bessel functions, when the flexural stiffness is negligible, i.e. for cables. A quite similar analysis is done by Senjanovic et al. [22], that better highlight the role of the "hypothetic tension force" and of the segmentation method they used. This work has been extended to the nonlinear regime in [23]. A numerical state-space approach is used in [24], where the results are validated with other, numerical and analytical, methods.

In the case of *uniformly* distributed axial load, and for any boundary conditions, an elegant closed form solution is obtained by Huang and Dareing [25, 26] by a power series, that however cannot be expressed in terms of known special functions (Bessel or others). Paidoussis [27] noted that 50 terms in the power series are needed to have an adequate accuracy (see also [24]).

In this paper, the Huang and Dareing [25, 26] solution is extended to *any arbitrarily* distributed axial load, and with the presence of a tip tension. In fact, to the best of the authors' knowledge, previous works always deal with uniformly distributed load or, equivalently, linearly varying axial force.

Furthermore, attention is focused on internal resonance [28, 29, 30], in particular on 1:3 resonance between the first and the second mode. The authors are not aware of previous papers dealing with internal resonance in beam with distributed axial loads.

This is motivated by its interest in practical applications. In fact, internal resonance, if not properly detected, may lead to unwanted dynamical behaviour due to nonlinear coupling, with unexpected activation of unforced natural modes, which may be dangerous for the structure. There is an hypothesis, supported by detailed arguments, that an internal resonance could be responsible for the famous collapse of the Tacoma Narrows Bridge [31].

Published online July 08 2020

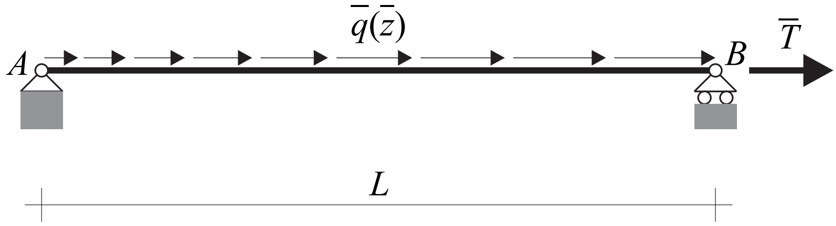

Fig. 1. The beam subject to distributed load and end traction.

2. The mechanical model

We consider the transversal, planar, linear vibrations of the Euler-Bernoulli beam reported in Fig. 1, which is subjected to an arbitrary distributed axial load $\bar{q}(\bar{z})$, to an end traction $\bar{T}$ and with generic boundary conditions (in Fig. 1 only the hinged-"hinged" case is reported for simplicity).

The equation of motion for the undamped free vibrations is (see eq. (11.178) of [11]):

$$\rho A\ddot{\bar{v}} + (EJ\bar{v}'')'' - (\bar{P}(\bar{z})\bar{v}')' = 0, \tag{1}$$

where $\bar{v}(\bar{z}, \bar{t})$ is the transversal displacement, L the length of the beam,

$$\bar{P}(\bar{z}) = \bar{T} + \int_{\bar{z}}^{L} \bar{q}(\bar{s})d\bar{s} \tag{2}$$

is the *given* internal axial force in the cross-section at distance $\bar{z}$ from the left end side A, and where the bending stiffness EJ and the mass per unit length ρA are constant since the beam is assumed to be homogenous and with constant cross-section. Dot means derivative with respect to time, and prime with respect to the spatial variable $\bar{z}$.

Since we are looking for free harmonic vibrations, it is customary to look for a solution in the form

$$\bar{v}(\bar{z}, \bar{t}) = v(\bar{z}) \sin(\omega\bar{t}). \tag{3}$$

where $v(\bar{z})$ is the mode shape and ω the natural (circular) frequency. The PDE (1) then becomes the ODE

$$-\omega^2 \rho A v + EJv^{IV} - (\bar{P}(\bar{z})v')' = 0. \tag{4}$$

It is useful to deal with a dimensionless version of (4). Defining

$$z = \frac{\bar{z}}{L},\ \lambda = \omega^2 \frac{\rho A\, L^4}{EJ},\ P(z) = \frac{\bar{P}(\bar{z})\, L^2}{EJ},\ T = \frac{\bar{T}\, L^2}{EJ},\ q(z) = \frac{\bar{q}(\bar{z})\, L^3}{EJ}, \tag{5}$$

the equation (4) becomes

$$-\lambda v + v^{IV} - (P(z)v')' = 0, \tag{6}$$

that will be considered in the following. Here $P(z) = T + \int_z^1 q(s)ds$ and λ is the square of the dimensionless frequency. Note that there is no need to adimensionalize v, since (6) is linear in v.

The *transversal* boundary conditions associated to (6), already in the dimensionless form, are

- hinged: $v = 0$ and $v'' = 0$;
- fixed: $v = 0$ and $v' = 0$;
- free: $v''' - Pv' = 0$ and $v'' = 0$;
- slider: $v''' - Pv' = 0$ and $v' = 0$,

to be applied at $z = 0$ and $z = 1$.

In the *axial* direction the beam is always fixed at $z = 0$ and the dimensionless traction force T is applied at $z = 1$ (see Fig. 1). However, the former boundary conditions is not explicitly required since we are considering the linear regime and the beam is straight, while the latter is implicitly considered in (2).

3. Power series solution

Since polynomials are dense, without loss of generality the arbitrary continuously distributed axial load $q(z)$ can be represented in the form

$$q(z) = \sum_{i=0}^{\infty} q_i z^i. \tag{7}$$

This suggests looking for the exact solution as a power series, too,

$$v(z) = \sum_{i=0}^{\infty} v_i z^i, \tag{8}$$

thus extending to the generic case $q(z)$ and $T \neq 0$ the same solution used in [25, 26] for the constant distributed load, $q(z) = q_0$.

Inserting (8) in (6), and using (7), we get the following recurrence relation between the coefficients v_n, $n \geq 0$:

$$\begin{aligned} v_{n+4} = & \frac{\lambda}{(n+4)(n+3)(n+2)(n+1)} v_n \\ & + \frac{1}{(n+4)(n+3)} \left(T + \sum_{k=0}^{\infty} \frac{q_k}{k+1} \right) v_{n+2} \\ & + \frac{1}{(n+4)(n+3)(n+2)} \sum_{k=0}^{n} q_k \frac{k-n-1}{k+1} v_{n+1-k}. \end{aligned} \tag{9}$$

Note that for $q(z) = 0$ the previous recurrence gives, depending on v_0, v_1, v_2 and v_3, trigonometric and hyperbolic sine and cosine functions.

By using (9), once v_0, v_1, v_2 and v_3 are given, the solution $v(z)$ is known by (8). Note that in general, even if $q(z)$ has a finite number of terms, the solution $v(z)$ has infinite terms. However, it can be easily approximated by a sufficiently large number N of terms in (8).

It is useful to consider four different cases:

$$\text{1) } v_0 = 1, v_1 = 0, v_2 = 0, v_3 = 0 \quad \rightarrow \quad g_0(z), \tag{10}$$
$$\text{such that } g_0(0) = 1,\ g_0'(0) = 0,\ g_0''(0) = 0,\ g_0'''(0) = 0,$$
$$\text{2) } v_0 = 0, v_1 = 1, v_2 = 0, v_3 = 0 \quad \rightarrow \quad g_1(z), \tag{11}$$
$$\text{such that } g_1(0) = 0,\ g_1'(0) = 1,\ g_1''(0) = 0,\ g_1'''(0) = 0,$$
$$\text{3) } v_0 = 0, v_1 = 0, v_2 = 1/2, v_3 = 0 \quad \rightarrow \quad g_2(z), \tag{12}$$
$$\text{such that } g_2(0) = 0,\ g_2'(0) = 0,\ g_2''(0) = 1,\ g_2'''(0) = 0,$$
$$\text{4) } v_0 = 0, v_1 = 0, v_2 = 0, v_3 = 1/6 \quad \rightarrow \quad g_3(z), \tag{13}$$
$$\text{such that } g_3(0) = 0,\ g_3'(0) = 0,\ g_3''(0) = 0,\ g_3'''(0) = 1,$$

so that the general solution can be written as the linear combination

$$v(z) = c_0\, g_0(z) + c_1\, g_1(z) + c_2\, g_2(z) + c_3\, g_3(z), \tag{14}$$

having the properties

$$v(0) = c_0, \quad v'(0) = c_1, \quad v''(0) = c_2, \quad v'''(0) = c_3. \tag{15}$$

Examples of the four functions $g_0(z)$, $g_1(z)$, $g_2(z)$ and $g_3(z)$, that depend on λ, $q(z)$ and T, are reported in Fig. 2.

By imposing the appropriate boundary conditions, we find a linear algebraic system of four equations in the four unknowns c_0, c_1, c_2 and c_3. Since the system is homogeneous, the non trivial solution is obtained by vanishing the determinant of the associated matrix. This leads to:

a) hinged-hinged: $g_1(1)g_3''(1) - g_3(1)g_1''(1) = 0$;
   $T_{cr} = -9.869604404 = -\pi^2$;

b) hinged-slider: $g_1'(1)g_3'''(1) - g_3'(1)g_1'''(1) = 0$;
   $T_{cr} = -2.467401101 = -(\pi/2)^2$;

c) fixed-fixed: $g_2(1)g_3'(1) - g_3(1)g_2'(1) = 0$;
   $T_{cr} = -39.47841762 = -(2\pi)^2$;

d) fixed-hinged: $g_2(1)g_3''(1) - g_3(1)g_2''(1) = 0$;
   $T_{cr} = -20.19972208 = -(\pi/0.699)^2$;

e) fixed-slider: $g_2(1)g_3'''(1) - g_3(1)g_2'''(1) = 0$;
   $T_{cr} = -9.869604404 = -\pi^2$;

f) fixed-free: $[g_2'(1)g_3''(1) - g_3'(1)g_2''(1)]T + [g_2''(1)g_3'''(1) - g_3''(1)g_2'''(1)] = 0$;
   $T_{cr} = -2.467401101 = -(\pi/2)^2$;

In the previous list the T_{cr}s are the classical Euler static ($\lambda = 0$) buckling loads without distributed load ($q(z) = 0$), that are reported for the sake of comparison with forthcoming results.

Solving the previous equations gives the λs (they are a countable infinity, but only the lower are interesting from a practical point of view) as a function of $q(z)$ and T. The associated modal shapes can then be obtained by determining the non trivial solution of the algebraic equations.

4. Results

We initially perform a convergence analysis to determine how many terms N are needed in (8) to have a sufficient accuracy. We report in Fig. 3 the ratio between the approximate and the "exact" (for $N = 100$) dimensionless natural frequencies for the hinged-hinged case and constant distributed load. It is possible to see that for $N = 45$ the convergence is reached (compare with the case $N = 50$ used in [27]). However, since it does not require an extra computational effort, in the following we will use $N = 100$.

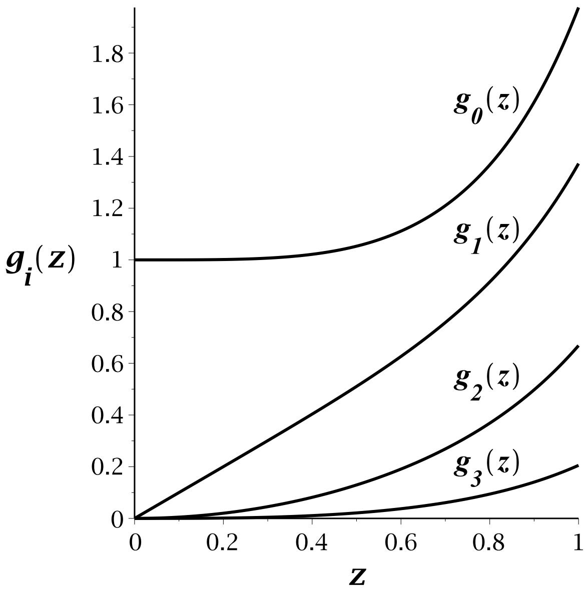

Fig. 2. The functions $g_0(z)$, $g_1(z)$, $g_2(z)$ and $g_3(z)$ for $\lambda = 20$, $T = 10$ and $q(z) = -20z + 4z^3$. $N = 100$ terms are used in the series (8).

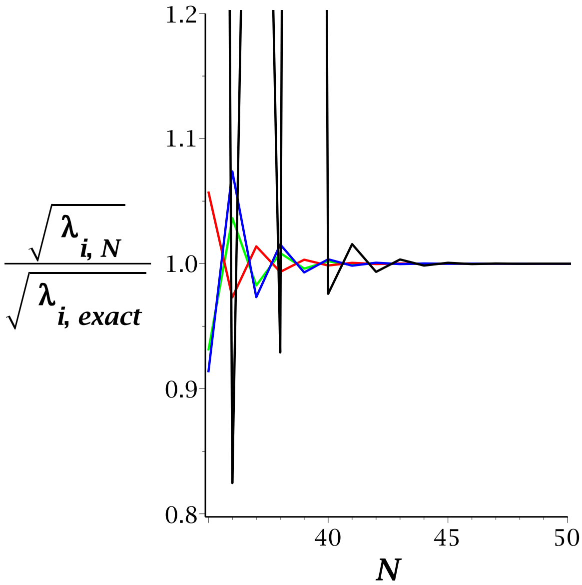

Fig. 3. The ratios between the approximate and the "exact" (for $N = 100$) dimensionless natural frequencies for increasing number of approximating terms N. Green=first mode, red=second mode, blue=third mode, black=fourth mode. $q(z) = 100$, $T = 0$, hinged-hinged boundary conditions.

4.1 Natural frequencies

In this section we report the natural frequencies for different boundary conditions, for $T = 0$ and for three different distributions of $q(z)$:

$$q(z) = q_0, \quad q(z) = 6\,q_1\,z(1-z), \quad q(z) = 3\,q_2 z^2. \tag{16}$$

Note that in all cases q_0, q_1 and q_2 represent the magnitude of the total load applied to the beam, i.e. the load resultant of the distributed load, so that the comparison between the three cases is easier. The only difference is in the distribution along the span, and in the position of the resultant ($L/2$ for the first two cases, $3L/4$ for the third case).

The first four natural frequencies for the constant distributed load $q(z) = q_0$ are reported in Fig. 4 by solid curves. Note that, as expected, the same results of [25, 26] have been obtained. The static buckling loads are those for which $\omega_1 = 0$, and are reported in Tab. 1.

The first four modal shapes for $q(z) = 100$, normalized by $\int_0^1 v(z)^2 dz = 1$, are reported in Fig. 5.

For the symmetric parabolic distributed axial load $q(z) = 6\,q_1\,z(1-z)$ the natural frequencies are reported by dashed curves in Fig. 4, while static buckling loads are reported in Tab. 2.

The dashdot curves of Fig. 4 correspond to the natural frequencies of the asymmetrical parabolic distributed load $q(z) = 3\,q_2\,z^2$. The static buckling loads are instead reported in Tab. 3.

Solid and dashed curves practically coincide in Fig. 4, namely there are minor differences between constant and symmetrical parabolic distributed axial loads. This means that the natural frequencies are not very much affected by the spatial distribution of the load (at least for the considered cases). On the other hand, there are some differences with the case of asymmetrical parabolic

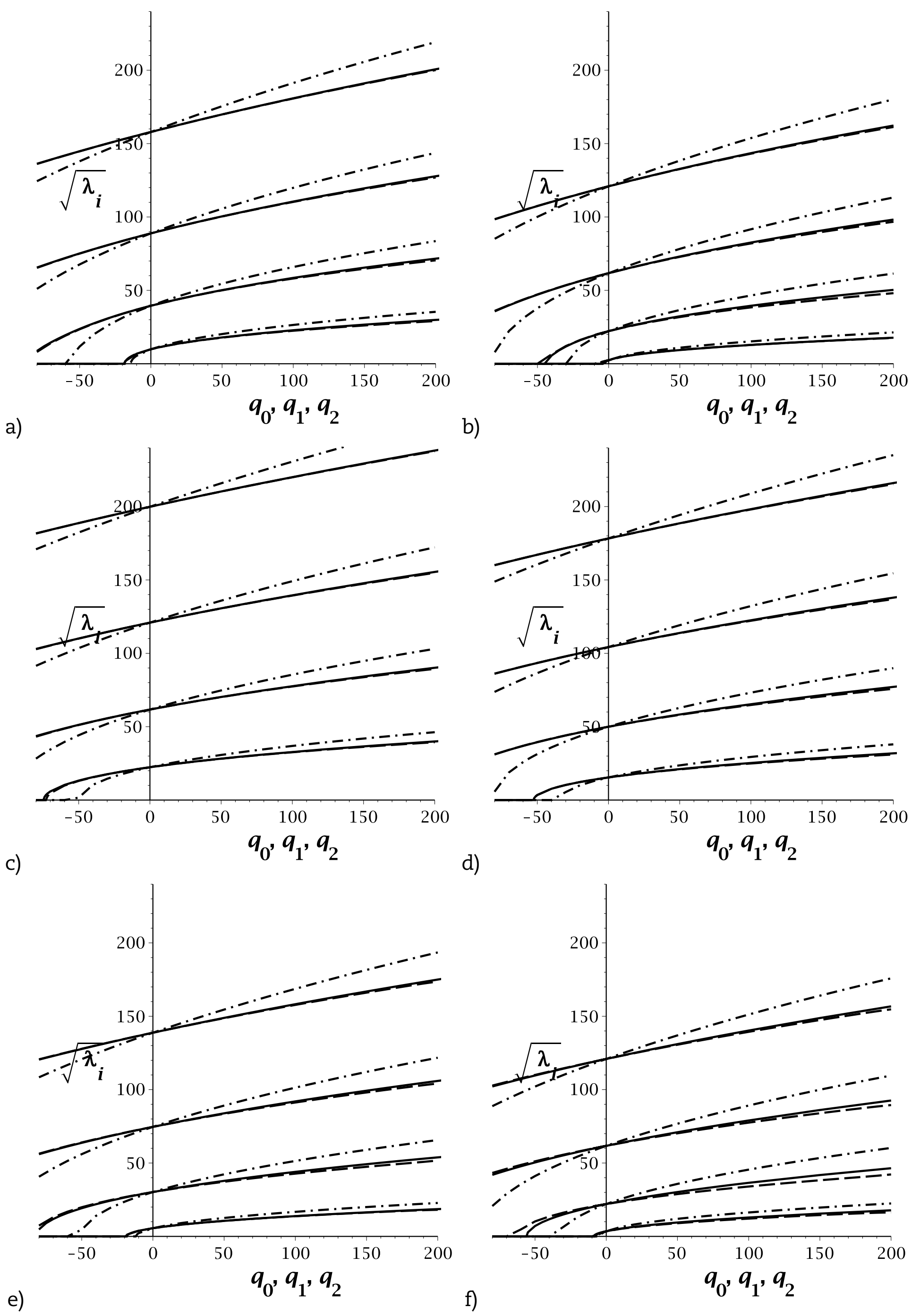

Fig. 4. The first four (dimensionless) natural frequencies for $q(z) = q_0$ (solid curves), for $q(z) = 6\,q_1\,z(1-z)$ (dashed curves) and for $q(z) = 3\,q_2\,z^2$ (dashdot curves). a) hinged-hinged, b) hinged-slider, c) fixed-fixed, d) fixed-hinged, e) fixed-slider, f) fixed-free. $T = 0$.

distributed axial loads (dashdot curve), i.e. the natural frequencies are instead influenced by the abscissa of the point of application of the resultant. In particular, for negative resultants the natural frequencies decrease when the resultant get closer to the boundary, while the ω_is increase for positive values of q_i.

Similar conclusions can be drawn for the buckling load (compare Tabs. 1, 2 and 3). We note that the buckling load decreases (in absolute value), when the resultant get closer to the boundary.

4.2 Internal resonances

Looking for internal resonances, the ratio between the second and the first natural frequencies is reported in Fig. 6, again by solid curves for constant distributed load, dashed curves for parabolic load and dashdot curves for asymmetrical parabolic load.

The most important internal resonances are 1:2, that may be activated in the presence of quadratic (asymmetric) nonlinearities, and 1:3, that my be activated by cubic (symmetric) nonlinear terms [32].

It is seen that 1:4 and 1:3 internal resonances occur for fixed values of the governing parameters, which are reported in Tabs. 1, 2 and 3. By varying the boundary conditions, the values of q_0, q_1 and q_2 for internal resonances vary, but the qualitative behaviour remains the same. Again, there are no major differences between constant and symmetrical parabolic distributed axial loads, while there are some differences with the asymmetrical parabolic load, due to the different position of the resultant.

The 1:2 and 1:1 internal resonances, on the other hand, have not been observed. Actually, 1:2 internal resonance can be observed when $q_0 \to \infty$; this can be easily understood, since in this case the beam becomes a string (the second order spatial derivative

	buckling	res. 1:4	res. 1:3
a) hinged-hinged	-18.57	0.00	30.91
b) hinged-slider	-3.48	26.76	123.79
c) fixed-fixed	-74.63	-51.60	-20.93
d) fixed-hinged	-52.50	-25.27	18.22
e) fixed-slider	-18.96	27.09	151.16
f) fixed-free	-7.84	18.21	70.12

Table 1. Critical values of q_0 for constant load $q(z) = q_0$, $T = 0$.

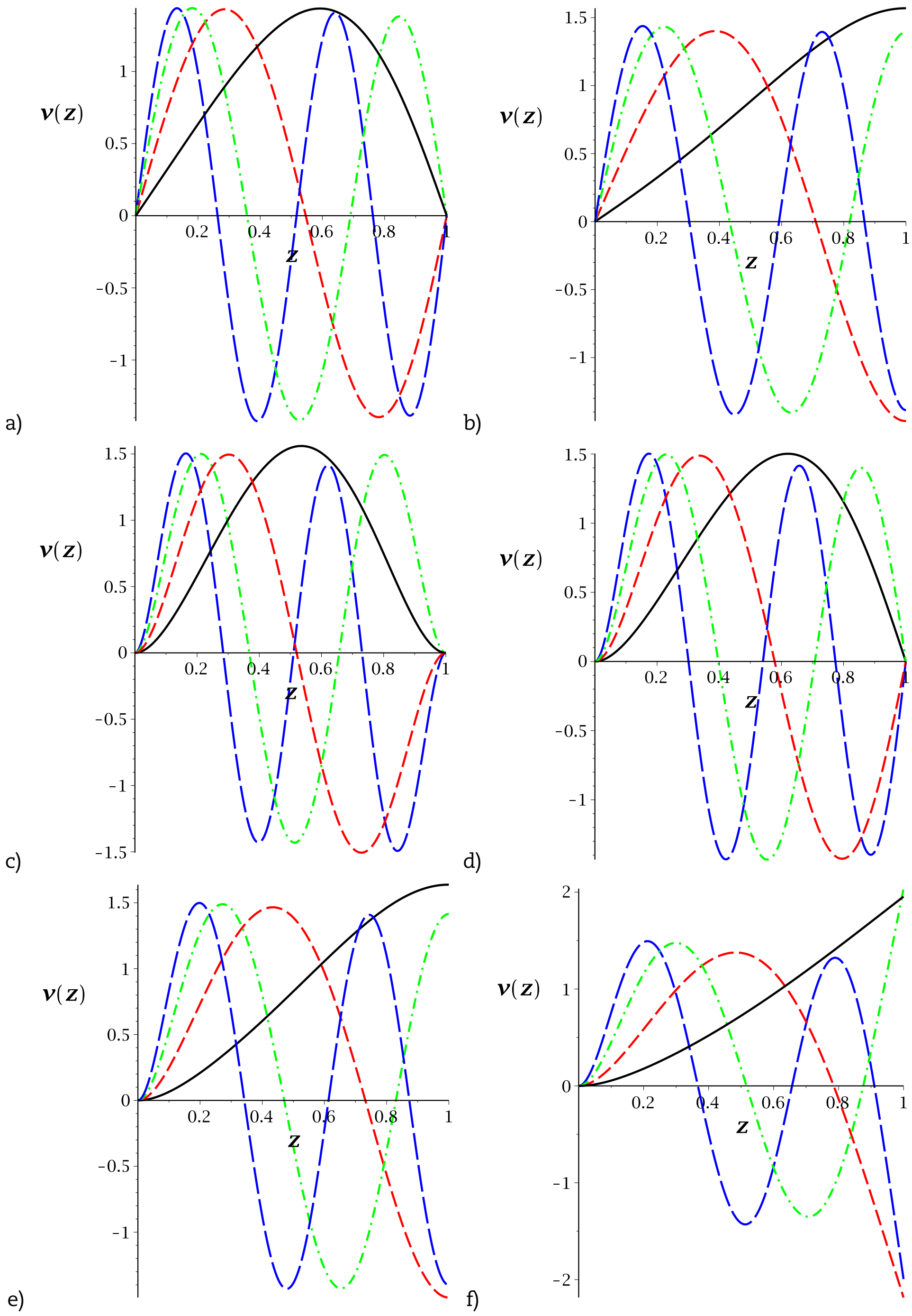

Fig. 5. The first (solid curves, black), second (dash curve, red), third (dashdot curve, green) and fourth (longdash curve, blue) normalized modal shapes for $q(z) = 100$. a) hinged-hinged, b) hinged-slider, c) fixed-fixed, d) fixed-hinged, e) fixed-slider, f) fixed-free. $T = 0$.

becomes dominant with respect to the fourth order) where it is well known the occurrence of this resonance. The reasoning is confirmed by the fact that all curves reported in Fig. 6 tend to 2 for $q_{0,1,2} \to \infty$.

	buckling	res. 1:4	res. 1:3
a) hinged-hinged	-18.34	0.00	31.75
b) hinged-slider	-3.26	24.09	97.74
c) fixed-fixed	-72.74	-50.84	-20.78
d) fixed-hinged	-52.32	-24.77	18.72
e) fixed-slider	-18.40	25.42	126.33
f) fixed-free	-8.71	19.22	69.22

Table 2. Critical values of q_1 for parabolic load $q(z) = 6\, q_1\, z(1-z)$, $T = 0$.

	buckling	res. 1:4	res. 1:3
a) hinged-hinged	-14.15	0.00	23.98
b) hinged-slider	-2.65	20.70	119.83
c) fixed-fixed	-50.24	-34.02	-13.81
d) fixed-hinged	-34.07	-15.44	12.13
e) fixed-slider	-11.82	18.10	125.88
f) fixed-free	-4.22	10.06	48.90

Table 3. Critical values of q_2 for asymmetrical parabolic load $q(z) = 3\, q_2\, z^2$, $T = 0$.

4.3 1:3 internal resonance

In the previous section we have seen the occurrence of the 1:3 internal resonance between the first and the second mode for all boundary conditions. Here this important phenomenon is deeply investigated, with the goal of determining its robustness by varying the distributed load $q(z)$ and the axial tension T.

We start with by considering constant load, $q(z) = q_0$, and varying the end traction T. For each T, the value of q_0 guaranteeing 1:3 internal resonance between the first and the second mode is reported in Fig. 7. The most important observation is that for any considered value of T there is always a q_0 providing 1:3 internal resonance. In other words, T is not able to destroy the occurrence of this dynamical phenomenon, but it just shifts it in the parameters space.

We observe that q_0 is a decreasing function of T; only for the fixed-free case, after initially decreasing, then it increases slowly, and we note that for $q_0 < 67$ there is no 1:3 internal resonance for any value of T. Actually, in the cases of hinged-slider and fixed-slider, the decrement of q_0 is very low, and, like for the fixed-free case, below a certain threshold ($q_0 < 110$ and $q_0 < 125$, respectively), there is no 1:3 internal resonance for every value of T.

It is interesting to note that the fixed-hinged case approaches the hinged-hinged case for negative (compression) values of T, while it approaches the fixed-fixed case for large tractions.

Let us now focus on the hinged-hinged case and consider a linearly distributed load, i.e. $q(z) = q_0 + q_1 z$. In the parameters plane (q_0, q_1), and for different values of T, the loci of points providing 1:3 internal resonance are reported in Fig. 8. Interestingly, the curves $q_1(q_0)$ are almost linear, and the slope barely depends on T.

Let us fix T, for example $T = 0$ (the thick curve of Fig. 8). The load corresponding to $q_1(q_0)$ of Fig. 8, namely $q(z) = q_0 + q_1(q_0)z$, are reported in Fig. 9. Surprisingly, all load distributions intersect in *practically* the same point, at $z_{cr} = -q_0/q_1 \cong 0.598$ for the value $q_{cr} = q(z_{cr}) = 30.78$ (note that $q_{cr} = q_0(q_1 = 0)$; it is also $q_0(T = 0)$ of Fig. 7 and, approximately, the value in the last column of Tab. 1), which is almost independent on the slope q_1. This is a very unexpected property, that allows us to conclude that any linear distributed load passing through q_{cr} at z_{cr} provides 1:3 internal resonance.

It should be noted that the intersection points are *not exactly the same*, but they are very close. For the case of Fig. 8 the 18 intersection points have average value $z_{cr} = 0.598$ and standard deviation $\sigma_z = 0.007266$. This latter is so small that practically we can consider the average value as the representative of all cases.

The property illustrated in Fig. 9 is *not* specific of hinged-hinged boundary conditions, nor of $T = 0$. Actually, behaviours qualitatively similar to that of Fig. 8 are observed for any boundary conditions and for any value of T. The functions $z_{cr}(T)$ are reported in Fig. 10. Note that the z_{cr} barely varies (apart from the fixed-free case, that confirms to be a little bit "different", see Fig. 7), and for increasing T it becomes almost constant.

The conclusion is that, for a fixed T, any linear distributed load having at z_{cr} given in Fig. 10 the value $q(z_{cr}) = q_0$ reported in Fig. 7, provides 1:3 internal resonance.

5. Conclusions and further developments

The free vibrations of a beam subjected to a generic distributed axial load have been investigated in depth. The *exact analytical* solution has been obtained in terms of a power series. A simple recurrence expression (eq. (9), valid for any boundary conditions) for the coefficients of the series has been proposed. It extends a previous solution valid only for uniformly distributed axial loads.

The general results have been illustrated by comparing the cases of constant and parabolic (symmetrical and asymmetrical) distributed loads, with no tip tension. It is shown that the natural frequency slightly depends on the shape of the distributed axial load, but mainly on their magnitude. In spite of this, however, it is expected that more complex spatial distribution of loads may affect significantly the natural frequencies.

The static buckling loads have also been determined in the previous cases.

Then, attention was paid to 1:3 internal resonance, and it has been shown that it is a robust phenomenon. In particular, its persistence for varying traction and for different linearly distributed axial load is illustrated.

A very unexpected property is found: when a linearly distributed load has a certain value at a certain abscissa (both depending on T and on boundary conditions, and determined in this work), any slope of the load leads to a 1:3 internal resonance.

An extension of the proposed solution to the case of varying bending stiffness and varying distributed mass, in addition to varying distributed axial load, can be easily foreseen by the same power series technique. Other possible developments concern experimental results confirming the present findings, in particular the 1:3 internal resonance; extension to the nonlinear regime (see [4] in this respect), in general and with specific attention to 1:3 internal resonance; optimization of distributed load for desired performance; exploitation of the proposed solution for specific practical applications.

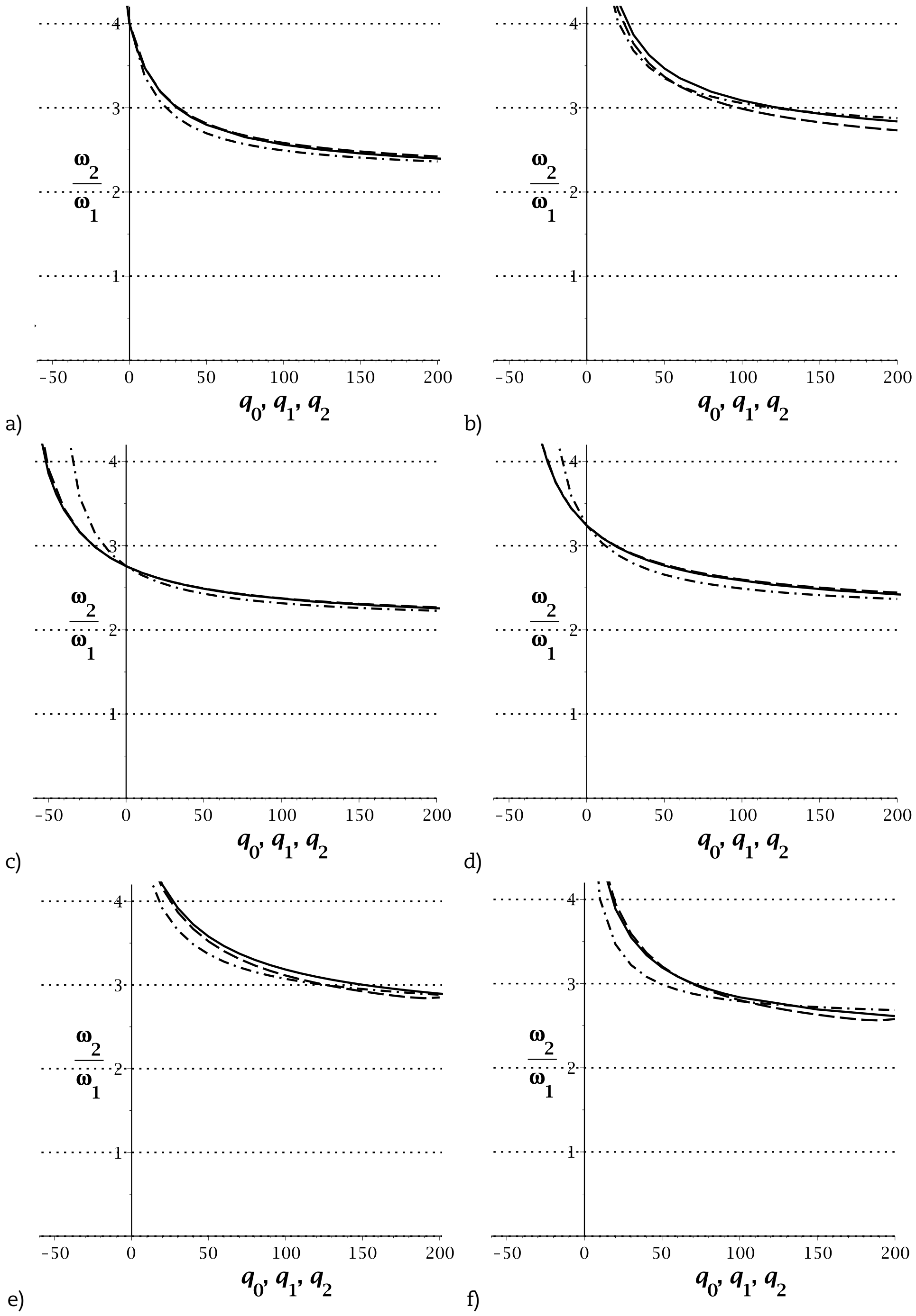

Fig. 6. The ratio between the second and first natural frequencies for $q(z) = q_0$ (solid curves), for $q(z) = 6\,q_1\,z(1-z)$ (dashed curves) and for $q(z) = 3\,q_2\,z^2$ (dashdot curves). a) hinged-hinged, b) hinged-slider, c) fixed-fixed, d) fixed-hinged, e) fixed-slider, f) fixed-free. $T = 0$.

Author Contributions

The authors declared to have contributed in equal parts to the work.

Conflict of Interest

The authors declared no potential conflicts of interest with respect to the research, authorship and publication of this article.

Funding

This work has been partially developed within the activities of the “Dipartimento di Eccellenza” granted by the DICEA, Polytechnic University of Marche. The work of SL is also a part of his activities for the CNR-INSEAN and for the GNFM.

References

[1] Patel, M.H., Seyed, F.B., Review of flexible riser modelling and analysis techniques, Eng. Structures, 17(4), 1995, 293-304.

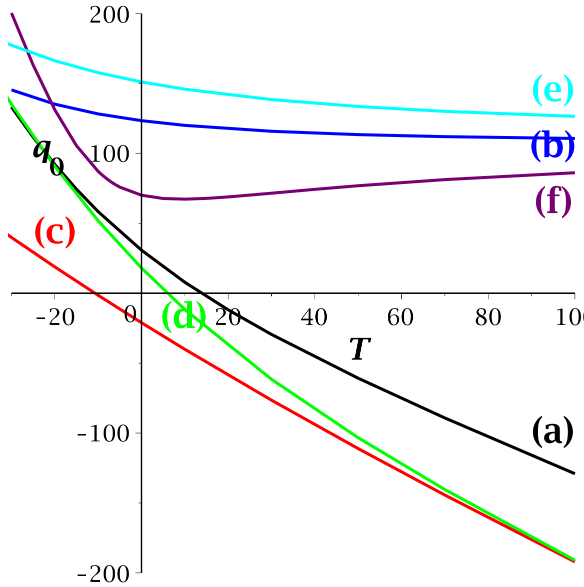

Fig. 7. The value of $q(z) = q_0$ guaranteeing 1:3 internal resonance between the first and the second mode as a function of T. a) hinged-hinged, b) hinged-slider, c) fixed-fixed, d) fixed-hinged, e) fixed-slider, f) fixed-free.

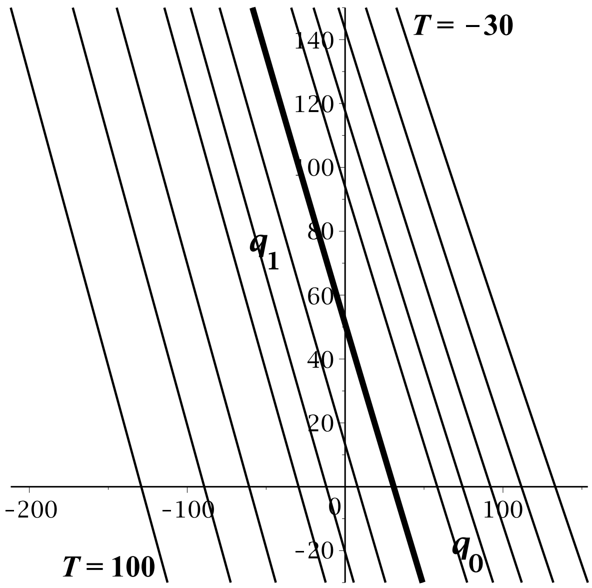

Fig. 8. The value of q_1 guaranteeing 1:3 internal resonance between the first and the second mode as a function of q_0 and for $T = -30; -25; -20; -15; -10; 0; 10; 20; 30; 50; 70; 100$. Hinged-hinged boundary conditions.

[2] Franzini, G.R., Santos, C.C.P., Mazzilli, C.E.N., Pesce, C.P., Parametric excitation of an immersed, vertical and slender beam using reduced-order models: influence of hydrodynamic coefficients, Marine Systems and Ocean Technology, 11(1-2), 2016, 10-18.
[3] Franzini, G.R., Mazzilli, C.E.N., Non-linear reduced-order model for parametric excitation analysis of an immersed vertical slender rod, Int. J. Non-Linear Mech., 80(1), 2016, 29-39.
[4] Vernizzi, G.J., Franzini, G.R., Lenci, S., Reduced-order models for the analysis of a vertical rod under parametric excitation, Int. J. Mech. Sciences, 163, 2019, 105122.
[5] Latalski, J., Warminski, J., Nonlinear vibrations of a rotating thin-walled composite piezo-beam with circumferentially uniform stiffness (CUS), Nonlinear Dynamics, 98(4), 2019, 2509-2529.
[6] Sterken, P., A guide for tree-stability analysis. No publisher, 2005. ISBN: 9090193774.
[7] Abdel-Gawwad, A.K., El-Kady, H.M., Shalaby, A.M., Three Dimensional Dynamic Analysis Of Ancient Egyptian Obelisks. To Investigate Their Behavior Under Aqaba Earthquake, J. Emerging Trends in Engineering and Applied Sciences, 2(2), 2011, 266-272.
[8] Virgin, L., Vibration of axially loaded structures, Cambridge University Press, 2007. ISBN-13 978-0-521-88042-8.
[9] Shaker, F.J., Effect of axial load on mode shapes and frequencies of beams, NASA Lewis Research Centre Report NASA-TN-8109, 1975.
[10] Timoshenko, S., Vibration problems in engineering, Nostrand, 1955.
[11] Rao, S.S., Vibrations of continuous systems, John Wiley & Sons, Hoboken, New Jersey, 2007. ISBN-13: 978-0-471-77171-5
[12] Bokaian, A., Natural frequencies of beams under compressive axial load, J. Sound Vibr., 126(1), 1988, 49-65.
[13] Bayon, A., Gascon, F., Medina, R., Nieves, F.J., Salazar, F.J., On the flexural vibration of cylinders under axial loads: Numerical and experimental study, J. Sound Vibr., 331(10), 2012, 2315-2333.
[14] Carpinteri, A., Malvano, R., Manuello, A., Piana, G., Fundamental frequency evolution in slender beams subjected to imposed axial displacements, J. Sound Vibr., 333, 2014, 2390-2403.
[15] Love, A.E.H., A treatise on the mathematical theory of elasticity, Dover Publication, 1944. ISBN 0-486-60174-9
[16] Villaggio, P., Mathematical models for elastic structures, Cambridge University Press, Pisa, 1997. ISBN: 0-521-57324-6

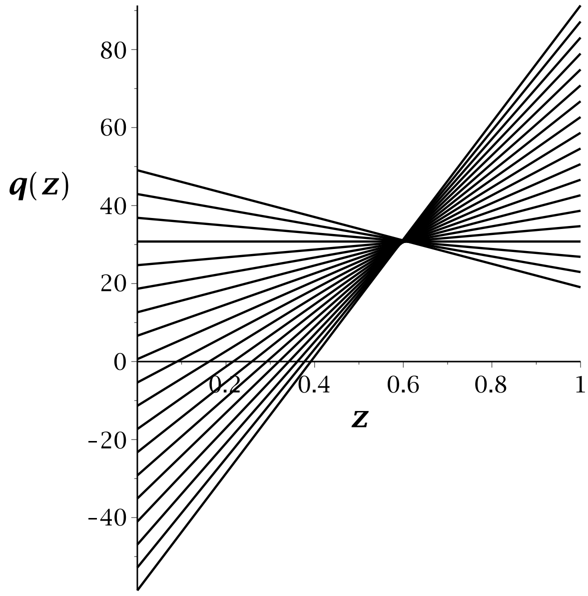

Fig. 9. The loads $q(z) = q_0 + q_1 z$ guaranteeing 1:3 internal resonance between the first and the second mode. $T = 0$ and hinged-hinged boundary conditions.

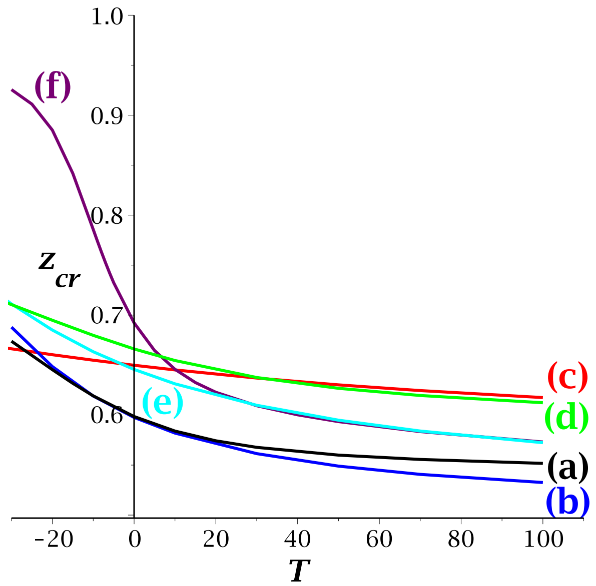

Fig. 10. The critical coordinate z_{cr} as a function of T. a) hinged-hinged, b) hinged-slider, c) fixed-fixed, d) fixed-hinged, e) fixed-slider, f) fixed-free.

[17] Greenhill, A.G., Determination of the greatest height consistent with stability that a vertical pole or mast can be made, and of the greatest height to which a tree of given proportion can grow, Cambridge Phil. Soc. Proc., 4, 1881, 65-73.
[18] Laird, W.M., Fauconneau, G., Upper and lower bounds for the eigenvalues of vibrating beams with linearly varying axial load. NASA-Cr-653, 1966.
[19] Pilkington, D.F, Carr, J.B., Vibration of beams subjected to end and axially distributed loading, J. Mech. Eng. Sci., 12, 1970, 70-72.
[20] Kim, Y.C., Natural frequencies and critical buckling loads of marine risers, J. Offshore Mech. Arct. Eng., 110(1), 1988, 2-8.
[21] Sparks, C.P., Transverse modal vibrations of vertical tensioned risers. A simplified analytical approach, Oil & Gas Science and Technology, 57(1), 2002, 71-86.
[22] Senjanovic, I., Ljusutina, A.M., Parunov, J., Natural vibration analysis of tensioned risers by segmentation method, Oil & Gas Science and Technology, 61(5), 2006, 647-659.
[23] Mazzilli, C.E.N., Lenci, S., Demeio, L., Non-linear free vibrations of tensioned vertical risers, in Ecker H., Steindl A., Jakubek S. (Eds) ENOC Proceeding of the 8th European Nonlinear Dynamics Conference, Vienna, Austria, 6-11 July 2014, 2014.
[24] Alfosail, F.K., Nayfeh, A.H., Younis, M.I., A state space approach for the eigenvalue problem of marine risers, Meccanica, 53, 2018, 747-757.
[25] Huang, T., Dareing, D.W., Buckling and lateral vibration of drill pipe, ASME J. Eng. for Industry, 90(4), 1968, 613-619.
[26] Huang, T., Dareing, D.W., Bucking and frequencies of long vertical pipes, ASCE J. Eng. Mechanics Division, 95(1), 1969, 167-181.
[27] Paidoussis, M., Dynamics of flexible slender cylinders in axial flow. Part 1. Theory, J. Fluid Mech., 26, 1966, 717–736.
[28] Bajaj, A.K., Davies, P., Chang, S.I., On internal resonances in mechanical systems, Chapter 3 of "Nonlinear Dynamics and Stochastic Mechanics", W. Kliemannin (Ed.), CRC Press, 1995 (e-version 2018). e-ISBN: 9781351075053.
[29] Manevich, A.I., Manevitch, L.I., Mechanics of nonlinear systems with internal resonances, Imperial College Press, 2003. ISBN: 978-1-86094-682-0.
[30] Clementi, F., Lenci, S., Rega, G., 1:1 internal resonance in a two d.o.f. complete system: a comprehensive analysis and its possible exploitation for design, Meccanica, 55, 2020, 1309-1332.
[31] Arioli, G., Gazzola, F., A new mathematical explanation of what triggered the catastrophic torsional mode of the Tacoma Narrows Bridge, Applied Mathematical Modelling, 39, 2015, 901–912.
[32] Nayfeh, A.H., Mook, D., Nonlinear oscillations, Wiley, 1979.

ORCID iD

Stefano Lenci https://orcid.org/0000-0003-3154-7896
Francesco Clementi https://orcid.org/0000-0002-9705-777X

How to cite this article: Stefano Lenci, Francesco Clementi. Natural frequencies and internal resonance of beams with arbitrarily distributed axial loads , J. Appl. Comput. Mech., 7(SI), 2021, 1009-1019. https://doi.org/10.22055/JACM.2020.32927.2104